Hindawi
Mathematical Problems in Engineering
Volume 2022, Article ID 3425073, 15 pages
https://doi.org/10.1155/2022/3425073

Research Article

Distributed Fixed-Time Coordinated Attitude Tracking Control with a Dynamic Leader for Spacecraft Formation Flying System

Zhanjie Zhou

Department of Control Science and Engineering, Harbin Institute of Technology, Harbin, Heilongjiang, China

Correspondence should be addressed to Zhanjie Zhou; hitzjz@163.com

Received 16 February 2022; Revised 28 March 2022; Accepted 12 April 2022; Published 17 June 2022

Academic Editor: Qingling Wang

This paper studies the problem of distributed coordinated attitude tracking control with a dynamic leader for spacecraft formation systems in the presence of parameter uncertainties and external disturbances. Under the constraint that the time-varying attitude trajectory of the leader is only available for a subset of the followers, a fixed-time distributed estimator for each follower is proposed. Moreover, a fixed-time distributed attitude tracking control law combined with a fixed-time distributed estimator and distributed adaptive control algorithm is proposed. This control law is dedicated to reducing the effects of system uncertainty and external bounded disturbances, and the settling time of this algorithm is independent of the initial state of the system. The fixed-time stability of the spacecraft formation system is proven with the Lyapunov-based approach, and numerical simulations clearly verify the effectiveness of the proposed control algorithm.

1. Introduction

With the development of science and technology, the scientific tasks undertaken by space technology have spread to many fields, including meteorology, geography, oceanography, communications, navigation, and space exploration. Moreover, scientific missions in the field of aerospace are becoming more complex and varied, and the traditional model of a single spacecraft working alone is no longer sufficient to satisfy the requirements of practical engineering. For this situation, the concept of spacecraft formation flying (SFF) was proposed. SFF carries several advantages in accomplishing space missions and creates new opportunities and applications for such missions [1]. As the basis for ensuring the realization of formation missions, coordinated attitude control, which can generally be categorized into centralized and distributed control, guarantees that the attitudes of spacecraft synchronize to a common value. Compared with traditional centralized coordination methods, distributed cooperative attitude control, which has the advantages of high efficiency, strong robustness, and high reliability, has received considerable attention.

Distributed cooperative attitude control can be divided into two cases: with a leader spacecraft and without a leader spacecraft. First, the coordinated attitude control of leaderless spacecraft formation systems is studied in [2, 3], where the attitude of each spacecraft synchronizes to a common value, which is an unknown quantity that is not set in advance. Because the desired trajectory of each spacecraft is identical, predefined, and time varying, Wu et al. [4] proposed a decentralized adaptive sliding-mode control algorithm that maintains synchronization of spacecraft attitudes in formation. Considering the existence of communication delay in spacecraft formation systems, Abdessameud et al. [5] presented an attitude synchronization scheme that solves this problem. Second, the case when there is a leader spacecraft in a spacecraft formation system is discussed. Coordinated attitude tracking control was investigated in [6], and the control algorithm guaranteed that the attitude of a follower spacecraft was asymptotically synchronized to the specified attitude of the leader spacecraft. In [7], a robust adaptive sliding-mode control strategy supported by a neural network with radial basis functions was developed, and attitude tracking was achieved with this adaptive

framework. However, all these methods in the mentioned literature only guarantee the asymptotic synchronization of a spacecraft's attitude. In [8, 9], a control law that can make a system achieve asymptotic stability was designed for the multiagent dynamic cooperative control problem with nonvanishing disturbances and time-varying networks, respectively.

Compared to asymptotic synchronization, finite-time synchronization implies faster application efficiency for SFF. The finite-time attitude synchronization problem for SFF is investigated in [10], and the control algorithm can ensure that the attitudes of spacecraft in the formation are synchronized in a finite time with zero final angular velocity. To improve the robustness of the system, a distributed attitude coordination control scheme using the terminal sliding mode (TSM) was proposed for a group of spacecrafts in the presence of external disturbances in [11], and the proposed control algorithm ensures that the system achieves finite-time stability. In [12–14], the finite-time algorithm was also applied, and the system obtained a faster convergence rate. The literature on finite-time cooperative attitude control algorithms for SFF is fruitful, but the settling time of finite-time control algorithms depends on the initial conditions of the system. The concept of fixed-time convergence, which ensures that the settling time is independent of the initial conditions, was proposed in [15]; thus, the settling times of fixed-time algorithms only depend on the design parameters. Based on fixed-time convergence theory, attitude control algorithms that can provide fixed-time convergence have been successively presented. Ning et al. [16] investigated the fixed-time coordinated tracking problem of nonlinear multiagent systems, and the settling time was directly estimated. A disturbance observer was employed in [17], and the observer combined with the fixed-time control algorithms effectively reduces the influence of external interference for a single spacecraft.

In addition to the convergence rate of a system, parameter uncertainties and external disturbances that affect the control performance and even undermine the stability of the system are another problem of coordinated attitude tracking control of spacecraft formations. In the presence of parametric uncertainties, a distributed adaptive control algorithm combined with distributed sliding-mode estimators was proposed in [18], and this approach can effectively reduce the effect of parametric uncertainties. In [19], a distributed adaptive control algorithm for reducing the influence of external interference combined with a distributed fixed-time sliding-mode control algorithm, which proved that the attitude error converges to the regions containing the origin in a fixed time, was proposed. Considering both parameter uncertainty and bounded external disturbances, a distributed adaptive control algorithm was proposed in [20]; however, this method can only guarantee the asymptotic stability of SFF. It is noted that the literature is unable to guarantee fixed-time stability for an SFF system with a dynamic leader in the presence of system uncertainties and external disturbances.

This study investigates the problem of distributed fixed-time attitude coordination tracking control with a dynamic leader for SFF in the presence of parameter uncertainties and bounded external disturbances. The objective is that the tracking attitude error of a group of follower spacecraft modeled by Euler–Lagrange equations converges to the regions containing the origin in a fixed time. The novel fixed-time controller designed in this study combined with fixed-time observers and adaptive algorithms that handle external disturbances and parameter uncertainties can effectively deal with the uncertainty of external disturbance and system inertia parameters. Since the convergence time of a fixed-time algorithm is independent of the initial system state, a fixed-time algorithm has wider application scenarios in practical engineering. Compared with existing works, the main contributions of this study are given as follows.

(1) In this study, only some follower spacecrafts can obtain the leader's attitude information. A fixed-time distributed estimator is employed to estimate the time-varying attitude trajectory of the leader for each spacecraft by using its neighbors' attitude information. The assumption that the leader's information is available for all follower spacecraft in [21, 22] is unnecessary. Compared with the traditional estimator in [20], the fixed-time estimator, which is independent of the initial conditions, provides faster application efficiency. The fixed-time estimator also provides a basis for the design of subsequent fixed-time attitude tracking control algorithms.

(2) Distributed adaptive control algorithms for both parameter uncertainties and bounded external disturbances, which are more general in the actual working environment of spacecraft, are designed. Compared with the algorithms that model a system only for the case of uncertainties or external disturbances in [18, 19, 23], the proposed algorithms in this study are more adapted to the actual situation. In particular, compared with [19, 23], the controller designed in this study can effectively deal with the inertia uncertainty of spacecraft.

(3) Combined with a fixed-time distributed estimator and distributed adaptive control algorithms, a fixed-time distributed attitude tracking control law is proposed. Compared with those in [11, 24], the distributed coordinated attitude tracking control algorithms, which are independent of the initial conditions designed in this study, guarantee that the attitude tracking error converges to the regions containing the origin in a fixed time. Combined with the fixed-time stability theory, the settling time of the system only depends on the controller parameters, and by choosing the appropriate parameters, the settling time can be designed to satisfy the requirements of practical applications.

Notations: $\otimes$ represents the Kronecker product. Given a vector $\mathbf{x} = [x_1, ..., x_n]^T$, we use $\|\mathbf{x}\|$ to denote the Euclidean norm and $\|\mathbf{x}\|_1$ represents the sum norm of the vector. For a vector $\mathbf{x}$, $\mathbf{x}^\alpha = [x_1^\alpha, ..., x_n^\alpha]^T$, $|\mathbf{x}|^\alpha = [|x_1|^\alpha, ..., |x_n|^\alpha]^T$, and $\mathrm{sig}^\alpha(\mathbf{x}) = [\mathrm{sgn}(x_1)|x_1|^\alpha, ..., \mathrm{sgn}(x_n)|x_n|^\alpha]^T$. For $\mathbf{x} =$

$[x_1, x_2, x_3]^T$, define $\mathbf{x}^\times = \begin{bmatrix} 0 & -x_3 & x_2 \\ x_3 & 0 & -x_1 \\ -x_2 & x_1 & 0 \end{bmatrix}$. $\lambda_{\min}(\mathbf{A})$ and $\lambda_{\max}(\mathbf{A})$ represent the minimum and maximum eigenvalues of matrix $\mathbf{A}$, respectively.

2. Background and Problem Statement

2.1. Spacecraft Attitude Dynamics. Consider a multiple rigid spacecraft system consisting of n followers, labeled spacecraft 1 to n, and one leader, labeled spacecraft 0. The attitude of the ith follower is described by modified Rodriguez parameters (MRPs) as

$$\dot{\sigma}_i = \mathbf{G}(\boldsymbol{\sigma}_i)\boldsymbol{\omega}_i, \tag{1}$$

where $\sigma_i = [\sigma_{i1}\ \sigma_{i2}\ \sigma_{i3}]^T \in R^3$ is the MRPs of the ith spacecraft denoting the attitude orientation of the body-fixed frame with respect to the inertial frame. $\omega_i \in R^3$ is the angular velocity of the ith rigid body with respect to the inertial frame, and $\mathbf{G}(\sigma_i)$ is expressed as

$$\mathbf{G}(\boldsymbol{\sigma}_i) = \frac{1}{2}\left[\frac{1-\|\boldsymbol{\sigma}_i\|^2}{2}\mathbf{I}_3 + \boldsymbol{\sigma}_i^\times + \boldsymbol{\sigma}_i\boldsymbol{\sigma}_i^T\right]. \tag{2}$$

The matrix $\mathbf{G}(\sigma_i)$ is provided with the following properties:

$$\det(\mathbf{G}(\boldsymbol{\sigma}_i)) = \frac{\left(1+\boldsymbol{\sigma}_i^T\boldsymbol{\sigma}_i^3\right)}{4} \neq 0, \tag{3a}$$

$$\mathbf{G}^T(\boldsymbol{\sigma}_i)\mathbf{G}(\boldsymbol{\sigma}_i) = \left(\frac{1+\boldsymbol{\sigma}_i^T\boldsymbol{\sigma}_i}{4}\right)^2\mathbf{I}_3. \tag{3b}$$

The dynamics of the ith spacecraft in the formation is described by

$$\mathbf{J}_i\dot{\omega}_i = -\boldsymbol{\omega}_i^\times\mathbf{J}_i\boldsymbol{\omega}_i + \mathbf{u}_i + \mathbf{t}_i, \tag{4}$$

where $\mathbf{J}_i \in R^{3\times3}$, $\mathbf{u}_i \in R^3$, and $\mathbf{t}_i \in R^3$ are the inertia matrix, control torque, and external disturbance torque of the ith spacecraft, respectively.

The n followers are represented with Euler–Lagrange equations by combining (1) and (4) as

$$\mathbf{M}_i(\boldsymbol{\sigma}_i)\ddot{\boldsymbol{\sigma}}_i + \mathbf{C}_i(\boldsymbol{\sigma}_i, \dot{\boldsymbol{\sigma}}_i)\dot{\boldsymbol{\sigma}}_i = \boldsymbol{\tau}_i + \mathbf{d}_i. \tag{5}$$

where $\mathbf{C}_i(\sigma_i, \dot{\sigma}_i) = -\mathbf{G}^{-T}(\sigma_i)\mathbf{J}_i\mathbf{G}^{-1}(\sigma_i)\ \dot{G}(\sigma_i)\mathbf{G}^{-1}(\sigma_i) - \mathbf{G}^{-T}(\sigma_i)\ (\mathbf{J}_i\omega_i)^\times\mathbf{G}^{-1}(\sigma_i)$, $\tau_i = \mathbf{G}^{-T}(\sigma_i)\mathbf{u}_i$, $\mathbf{d}_i = \mathbf{G}^{-T}(\sigma_i)\mathbf{t}_i$, and $\mathbf{M}_i(\sigma_i) = \mathbf{G}^{-T}(\sigma_i)\mathbf{J}_i\mathbf{G}^{-1}(\sigma_i)$. According to (3a) and (3b), $\mathbf{M}_i(\sigma_i)$ is the symmetric positive definite inertia matrix. Throughout the subsequent analysis, the following fundamental properties of system (5) are given in [25]

Property 1 (parameter boundedness). for any ith spacecraft, there exist positive constants k_m, k_M, and k_C, where $0 < k_m\mathbf{I}_3 \leq \mathbf{M}_i(\sigma_i) \leq k_M\mathbf{I}_3$ and $\|\mathbf{C}_i(\sigma_i, \dot{\sigma}_i)\| \leq k_C\|\dot{\sigma}_i\|$.

Property 2. (linearity in the dynamic parameters). $\mathbf{M}_i(\sigma_i)x + \mathbf{C}_i(\sigma_i, \dot{\sigma}_i)y = \mathbf{Y}_i(\sigma_i, \dot{\sigma}_i, x, y)\Theta_i$ for any x and $y \in R^3$, where Θ_i is the constant parameters vector associated with the ith spacecraft and $\mathbf{Y}_i(\sigma_i, \dot{\sigma}_i, x, y)\Theta_i$ is a known regression matrix.

Assumption 1. The time-varying state quantities of the leader spacecraft σ_0, $\dot{\sigma}_0$, and $\ddot{\sigma}_0$ are bounded.We assume $|\dot{\sigma}_{0m}| \leq \delta_1$ and $|\ddot{\sigma}_{0m}| \leq \delta_2$, where $m = 1, 2, 3$.

Assumption 2. The external disturbance torque $\mathbf{d}_i$ has an unknown upper bound; we assume $|d_{im}| \leq k_i$, where $i = 1, 2, \ldots, n$ and $m = 1, 2, 3$.

2.2. Graph Theory. To represent the topology of the information flow among spacecraft in the formation, graph theory is briefly introduced. An undirected weighted graph can be denoted as $G = (\mathbf{N}, \mathbf{E}, \mathbf{A})$, where $\mathbf{N} = (n_0, n_1, \ldots, n_n)$ is a finite nonempty set of nodes and $\mathbf{E} \subseteq \mathbf{N} \times \mathbf{N}$ is a set of unordered pairs of nodes. An edge $(n_i, n_j) \in \mathbf{E}$ denotes that the jth spacecraft can obtain the information from the ith spacecraft and vice versa. The adjacency matrix $\mathbf{A} = [a_{ij}] \in R^{n\times n}$ of graph G is defined such that adjacency elements a_{ij} satisfy $a_{ij} = 1$ if $(n_i, n_j) \in \mathbf{E}$, and $a_{ij} = 0$ otherwise. The Laplacian matrix $\mathbf{L} = [l_{ij}] \in R^{n\times n}$ associated with $\mathbf{A}$ is defined as $l_{ii} = \sum_{i\neq j} a_{ij}$ and $l_{ij} = -a_{ij}$, where $i \neq j$. The leader adjacency matrix is defined as $\mathbf{B} = \operatorname{diag}(a_{10}, a_{20}, \ldots, a_{n0})$, where $a_{i0} = 1$ if the ith spacecraft can obtain the information from the leader, and $a_{i0} = 0$ otherwise. Here, $\mathbf{H} = \mathbf{L} + \mathbf{B}$. Obviously, $\mathbf{L}$ and $\mathbf{H}$ are symmetric matrices.

Lemma 1 (see [26]). *If the graph $\overline{G}$ is an undirected connected graph, then all eigenvalues of the matrix $\mathbf{L}$ have an ascending order, where $0 = \lambda_1 < \lambda_2 \leq \lambda_3 \leq \cdots \leq \lambda_n$.*

Lemma 2 (see [27]). *If the graph $\overline{G}$ is an undirected connected graph, then the matrix $\mathbf{H}$ is a symmetric matrix, and all eigenvalues of the matrix $\mathbf{H}$ are positive.*

2.3. Mathematic Background. Consider the following system:

$$\dot{x} = g(t, x), x(0) = x_0, \tag{6}$$

where $x \in R^n$ and g: $R_+ \times R^n \longrightarrow R^n$ is a nonlinear function that can be discontinuous. For system (6), the following definitions and lemmas are given.

Definition 1 (see [15]). The equilibrium of system (6) is fixed-time stable if it is finite-time stable, and the settling time $T(x_0)$ is uniformly bounded for any initial state, that is, $\exists T_{\max} > 0$ such that $T(x_0) \leq T_{\max}$, where $\forall x_0 \in R^n$.

Lemma 3 (see [15]). *If there exists a continuous radially unbounded function V: $R^n \longrightarrow R_+ \cup \{0\}$ such that*

(1) $V(x) = 0 \Leftrightarrow x = 0$.

(2) For any solution $x(t)$ of (6) satisfies the inequality $D^*V(x(t)) \leq -(\alpha V^p(x(t)) + \beta V^q(x(t)))^k$ for some

$\alpha, \beta, p, q, k > 0$: $pk < 1, qk > 1$, then the origin is globally fixed-time stable for system (6) and the following estimate holds:

$$T(x_0) \le \frac{1}{\alpha^k (1 - pk)} + \frac{1}{\beta^k (qk - 1)} \quad \forall x_0 \in R^n, \tag{7}$$

where $D^* f(t) = \lim_{h \longrightarrow 0+} \sup (f(t+h) - f(t))/h$.

Lemma 4 (see [28]). *Let $\xi_1, \xi_2, \ldots, \xi_n \ge 0$. Then,*

$$\sum_{i=1}^{n} \xi_i^p \ge \left(\sum_{i=1}^{n} \xi_i \right)^p, \quad \text{if } 0 < p \le 1, \sum_{i=1}^{n} \xi_i^p \ge n^{1-p} \left(\sum_{i=1}^{n} \xi_i \right)^p, \quad \text{if } p > 1. \tag{8}$$

Lemma 5 (see [29]). *For any $\mathbf{a}, \mathbf{b} \in R^n$ and any symmetric positive definite matrix $\Phi \in R^{n \times n}$,*

$$2\mathbf{a}^T \mathbf{b} \le \mathbf{a}^T \Phi^{-1} \mathbf{a} + \mathbf{b}^T \Phi \mathbf{b}. \tag{9}$$

2.4. Problem Statement. Consider an SFF system consisting of n followers, which are described by (5), and a leader spacecraft. The leader's attitude information is only available for a some of the follower spacecraft under an undirected communication graph $\overline{G}$. The attitude tracking error and its derivative for each follower spacecraft is defined as

$$\mathbf{e}_{1i} = \boldsymbol{\sigma}_i - \boldsymbol{\sigma}_0, \tag{10}$$

$$\mathbf{e}_{2i} = \dot{\boldsymbol{\sigma}}_i - \dot{\boldsymbol{\sigma}}_0. \tag{11}$$

This study aims to design a distributed attitude control algorithm τ_i for each follower spacecraft in the presence of parameter uncertainties and external disturbances such that all spacecraft attitudes achieve synchronization, which means that $\mathbf{e}_{1i}$ and $\mathbf{e}_{2i}$ converge to the regions containing the origin in a fixed time.

3. Distributed Fixed-Time Coordinated Attitude Tracking Control

3.1. Fixed-Time Distributed Estimator Design. In this section, since only some of the following spacecraft can obtain the attitude information of the leader, to achieve attitude synchronization, state estimators dedicated to obtaining accurate estimates of σ_0 and $\dot{\sigma}_0$ for each follower based on fixed-time convergence theory are designed. The estimators are designed as

$$\begin{aligned} \dot{\hat{\boldsymbol{\sigma}}}_i &= -\alpha_1 \operatorname{sign}^{r_1} \left[\sum_{j=1}^{n} a_{ij} \left(\hat{\boldsymbol{\sigma}}_i - \hat{\boldsymbol{\sigma}}_j \right) + a_{i0} \left(\hat{\boldsymbol{\sigma}}_i - \boldsymbol{\sigma}_0 \right) \right] - \alpha_2 \operatorname{sign}^{r_2} \left[\sum_{j=1}^{n} a_{ij} \left(\hat{\boldsymbol{\sigma}}_i - \hat{\boldsymbol{\sigma}}_j \right) + a_{i0} \left(\hat{\boldsymbol{\sigma}}_i - \boldsymbol{\sigma}_0 \right) \right] \\ &= -\beta_1 \operatorname{sign} \left[\sum_{j=1}^{n} a_{ij} \left(\hat{\boldsymbol{\sigma}}_i - \hat{\boldsymbol{\sigma}}_j \right) + a_{i0} \left(\hat{\boldsymbol{\sigma}}_i - \boldsymbol{\sigma}_0 \right) \right], \end{aligned} \tag{12}$$

$$\begin{aligned} \dot{\hat{\mathbf{v}}}_i &= -\alpha_1 \operatorname{sign}^{r_1} \left[\sum_{j=1}^{n} a_{ij} \left(\hat{\mathbf{v}}_i - \hat{\mathbf{v}}_j \right) + a_{i0} \left(\hat{\mathbf{v}}_i - \dot{\boldsymbol{\sigma}}_0 \right) \right] - \alpha_2 \operatorname{sign}^{r_2} \left[\sum_{j=1}^{n} a_{ij} \left(\hat{\mathbf{v}}_i - \hat{\mathbf{v}}_j \right) + a_{i0} \left(\hat{\mathbf{v}}_i - \dot{\boldsymbol{\sigma}}_0 \right) \right] \\ &= -\beta_2 \operatorname{sign} \left[\sum_{j=1}^{n} a_{ij} \left(\hat{\mathbf{v}}_i - \hat{\mathbf{v}}_j \right) + a_{i0} \left(\hat{\mathbf{v}}_i - \dot{\boldsymbol{\sigma}}_0 \right) \right], \end{aligned} \tag{13}$$

where $\hat{\sigma}_i$ is the estimate of σ_0 and $\hat{v}_i$ is the estimate of $\dot{\sigma}_0$, $\alpha_1 > 0$, $\alpha_2 > 0$, $0 < \gamma_1 < 1$, $\gamma_2 > 1$, $\beta_1 \ge \delta_1$, and $\beta_2 \ge \delta_2$.

The errors of the estimated states are defined as

$$\tilde{\boldsymbol{\sigma}}_i = \hat{\boldsymbol{\sigma}}_i - \boldsymbol{\sigma}_0, \tag{14}$$

$$\tilde{v}_i = \hat{v}_i - \dot{\boldsymbol{\sigma}}_0. \tag{15}$$

Theorem 1. *Considering the spacecraft formation attitude system (5) under an undirected connected communication graph $\overline{\mathbf{G}}$. $\tilde{\sigma}_i$ and $\tilde{\mathbf{v}}_i$ converge to zero in a fixed time with a settling time $T_1 \le (2^{(1-\gamma_1)/2}/\alpha_1 [\lambda_{\min}(H)]^{(1-\gamma_1)/2} (1 - \gamma_1)) + ((2/3n)^{(1-\gamma_2)/2}/\alpha_2 [\lambda_{\min}(H)]^{(\gamma_2+1)/2} (\gamma_2 - 1))$ by estimators (12) and (13) under Assumption 1.*

Proof. Define $\tilde{\sigma} = [\tilde{\sigma}_1^T, \tilde{\sigma}_2^T, \ldots, \tilde{\sigma}_n^T]^T$. Based on Lemma 2, the Lyapunov function is described as

$$V_1 = \frac{1}{2}\tilde{\boldsymbol{\sigma}}^T(\mathbf{H}\otimes\mathbf{I}_3)\tilde{\boldsymbol{\sigma}}. \tag{16}$$

Taking the time derivative of the Lyapunov function V_1, we have

$$\begin{aligned}\dot{V}_1 &= \tilde{\boldsymbol{\sigma}}^T(\mathbf{H}\otimes\mathbf{I}_3)\left(\dot{\tilde{\boldsymbol{\sigma}}} - \mathrm{I}_n\otimes\dot{\boldsymbol{\sigma}}_0\right)\\ &= -\alpha_1\tilde{\boldsymbol{\sigma}}^T(\mathbf{H}\otimes\mathbf{I}_3)\mathrm{sig}^{r_1}\left[(\mathbf{H}\otimes\mathbf{I}_3)\tilde{\boldsymbol{\sigma}}\right]\\ &\quad -\alpha_2\tilde{\boldsymbol{\sigma}}^T(\mathbf{H}\otimes\mathbf{I}_3)\mathrm{sig}^{r_2}\left[(\mathbf{H}\otimes\mathbf{I}_3)\tilde{\boldsymbol{\sigma}}\right]\\ &= -\beta_1\tilde{\boldsymbol{\sigma}}^T(\mathbf{H}\otimes\mathbf{I}_3)\mathrm{sign}\left[(\mathbf{H}\otimes\mathbf{I}_3)\tilde{\boldsymbol{\sigma}}\right] - \tilde{\boldsymbol{\sigma}}^T(\mathbf{H}\otimes\mathbf{I}_3)(\mathrm{I}_n\otimes\dot{\boldsymbol{\sigma}}_0).\end{aligned} \tag{17}$$

Define $\mathbf{P} = (\mathbf{H}\otimes\mathbf{I}_3)\tilde{\sigma} = [p_{11}, p_{12}, p_{13}, \ldots, p_{n1}, p_{n2}, p_{n3}]^T$. Based on Lemma 4, we obtain

$$\begin{aligned}\dot{V}_1 &= -\alpha_1\sum_{i=1}^{n}\sum_{m=1}^{3}\left(p_{im}^2\right)^{(\gamma_1+1)/2} - \alpha_2\sum_{i=1}^{n}\sum_{m=1}^{3}\left(p_{im}^2\right)^{(\gamma_2+1)/2} - \beta_1\sum_{i=1}^{n}\sum_{m=1}^{3}\left|p_{im}\right| - \sum_{i=1}^{n}\sum_{m=1}^{3}p_{im}\dot{\sigma}_{0m}\\ &\le -\alpha_1\left[\sum_{i=1}^{n}\sum_{m=1}^{3}\left(p_{im}^2\right)\right]^{(\gamma_1+1)/2} - \alpha_2(3n)^{(1-\gamma_2)/2}\left[\sum_{i=1}^{n}\sum_{m=1}^{3}\left(p_{im}^2\right)\right]^{(\gamma_2+1)/2} - \beta_1\sum_{i=1}^{n}\sum_{m=1}^{3}\left|p_{im}\right| - \sum_{i=1}^{n}\sum_{m=1}^{3}p_{im}\dot{\sigma}_{0m}\\ &\le -\alpha_1\left(\|\mathbf{P}\|^2\right)^{(\gamma_1+1)/2} - \alpha_2(3n)^{(1-\gamma_2)/2}\left(\|\mathbf{P}\|^2\right)^{(\gamma_2+1)/2} - \beta_1\sum_{i=1}^{n}\sum_{m=1}^{3}\left|p_{im}\right| - \sum_{i=1}^{n}\sum_{m=1}^{3}p_{im}\dot{\sigma}_{0m}\\ &\le -\alpha_1\left(\|\mathbf{P}\|^2\right)^{(\gamma_1+1)/2} - \alpha_2(3n)^{(1-\gamma_2)/2}\left(\|\mathbf{P}\|^2\right)^{(\gamma_2+1)/2} - (\beta_1-\delta_1)\sum_{i=1}^{n}\sum_{m=1}^{3}\left|p_{im}\right|\\ &\le -\alpha_1\left[2\lambda_{\min}(\mathbf{H})\right]^{\gamma_1+1/2}(V_1)^{(\gamma_1+1)/2} - \alpha_2(3n)^{(1-\gamma_2)/2}\left[2\lambda_{\min}(\mathbf{H})\right]^{(\gamma_2+1)/2}(V_1)^{(\gamma_2+1)/2}.\end{aligned} \tag{18}$$

According to Lemma 3, $\tilde{\sigma}_i$ converges to zero in a fixed time with a settling time T_1, which is described as

$$\begin{aligned}T_1 \le &\frac{2^{(1-\gamma_1)/2}}{\alpha_1\left[\lambda_{\min}(\mathbf{H})\right]^{(\gamma_1+1)/2}(1-\gamma_1)}\\ &+\frac{(2/3n)^{(1-\gamma_2)/2}}{\alpha_2\left[\lambda_{\min}(\mathbf{H})\right]^{(\gamma_2+1)/2}(\gamma_2-1)}.\end{aligned} \tag{19}$$

The proof process for the two estimators is similar. This completes the proof of Theorem 1. □

Remark 1. According to Lemma 2, the matrix $\mathbf{H}$ is a positive definite symmetric matrix; then, there is certainly an orthogonal matrix $\mathbf{U}$ such that

$$\begin{aligned}\|\mathbf{P}\|^2 &= \mathbf{P}^T\mathbf{P} = \tilde{\boldsymbol{\sigma}}^T(\mathbf{H}\otimes\mathbf{I}_3)(\mathbf{H}\otimes\mathbf{I}_3)\tilde{\boldsymbol{\sigma}}\\ &= \tilde{\boldsymbol{\sigma}}^T\mathbf{U}^T\mathrm{diag}\left(\lambda_1^2, \lambda_2^2, \ldots, \lambda_{3n}^2\right)\mathbf{U}\tilde{\boldsymbol{\sigma}} = \sum_{i=1}^{3n}\lambda_i^2 b_i^2,\end{aligned} \tag{20}$$

$$\begin{aligned}V_1 &= \frac{1}{2}\tilde{\boldsymbol{\sigma}}^T(\mathbf{H}\otimes\mathbf{I}_3)\tilde{\boldsymbol{\sigma}} = \frac{1}{2}\tilde{\boldsymbol{\sigma}}^T\mathbf{U}^T\mathrm{diag}(\lambda_1, \lambda_2, \ldots, \lambda_{3n})\mathbf{U}\tilde{\boldsymbol{\sigma}}\\ &= \frac{1}{2}\sum_{i=1}^{3n}\lambda_i b_i^2.\end{aligned} \tag{21}$$

Then, we can obtain

$$2\lambda_{\min}(\mathbf{H})V_1 \le \|\mathbf{P}\|^2 \le 2\lambda_{\max}(\mathbf{H})V_1, \tag{22}$$

where $\mathbf{b} = \mathbf{U}\tilde{\sigma} = [b_1, b_1, \ldots, b_{3n}]^T$ and λ_i is the eigenvalue of matrix $\mathbf{H} \otimes \mathbf{I}_3$, and based on the property of Kronecker product, $\lambda_{\min}(\mathbf{H} \otimes \mathbf{I}_3) = \lambda_{\min}(\mathbf{H})$ and $\lambda_{\max}(\mathbf{H} \otimes \mathbf{I}_3) = \lambda_{\max}(\mathbf{H})$.

3.2. Fixed-Time Distributed Coordinated Adaptive Attitude Tracking Control Algorithm Design. In this section, the fixed-time distributed coordinated adaptive attitude tracking control algorithm is designed based on the fixed-time distributed estimator designed in the previous section.

The attitude state errors between the ith and jth spacecraft are defined by

$$\mathbf{e}_{1ij} = \boldsymbol{\sigma}_i - \boldsymbol{\sigma}_j, \tag{23}$$

$$\mathbf{e}_{2ij} = \dot{\boldsymbol{\sigma}}_i - \dot{\boldsymbol{\sigma}}_j. \tag{24}$$

The lumped attitude state errors are defined as

$$\begin{aligned}\boldsymbol{\theta}_{1i} &= \sum_{j=1}^{n} a_{ij}\mathbf{e}_{1ij} + \mathbf{e}_{1i} \\ &= \sum_{j=1}^{n} a_{ij}\left(\boldsymbol{\sigma}_i - \boldsymbol{\sigma}_j\right) + \left(\boldsymbol{\sigma}_i - \boldsymbol{\sigma}_0\right) \\ &= \sum_{j=1}^{n} a_{ij}\left[\left(\boldsymbol{\sigma}_i - \boldsymbol{\sigma}_0\right) - \left(\boldsymbol{\sigma}_j - \boldsymbol{\sigma}_0\right)\right] + \left(\boldsymbol{\sigma}_i - \boldsymbol{\sigma}_0\right),\end{aligned} \tag{25}$$

$$\begin{aligned}\boldsymbol{\theta}_{2i} &= \sum_{j=1}^{n} a_{ij}\mathbf{e}_{2ij} + \mathbf{e}_{2i} \\ &= \sum_{j=1}^{n} a_{ij}\left(\dot{\boldsymbol{\sigma}}_i - \dot{\boldsymbol{\sigma}}_j\right) + \left(\dot{\boldsymbol{\sigma}}_i - \dot{\boldsymbol{\sigma}}_0\right) \\ &= \sum_{j=1}^{n} a_{ij}\left[\left(\dot{\boldsymbol{\sigma}}_i - \dot{\boldsymbol{\sigma}}_0\right) - \left(\dot{\boldsymbol{\sigma}}_j - \dot{\boldsymbol{\sigma}}_0\right)\right] + \left(\dot{\boldsymbol{\sigma}}_i - \dot{\boldsymbol{\sigma}}_0\right).\end{aligned} \tag{26}$$

Here, $\mathbf{e}_1 = [\mathbf{e}_{11}^T, \mathbf{e}_{12}^T, \ldots, \mathbf{e}_{1n}^T]^T$, $\mathbf{e}_2 = [\mathbf{e}_{21}^T, \mathbf{e}_{22}^T, \ldots, \mathbf{e}_{2n}^T]^T$, $\theta_1 = [\theta_{11}^T, t\theta_{12}^T n, q \ldots h, {}_\theta 1n^T]^T = [(\mathbf{L} + \mathbf{I}_n) \otimes t\mathbf{I}_3]\mathbf{e}_1$, and $\theta_2 = [\theta_{21}^T, \theta_{22}^T, \ldots, \theta_{2n}^T]^T = [(\mathbf{L} + \mathbf{I}_n) \otimes \mathbf{I}_3]\mathbf{e}_2$. Based on Lemma 2, $\mathbf{L} + \mathbf{I}_n$ is a symmetric positive definite inertia matrix.

An auxiliary variable $\dot{\sigma}_{ri}$ is constructed as

$$\begin{aligned}\dot{\boldsymbol{\sigma}}_{ri} &= \hat{\mathbf{v}}_i - \sum_{j=1}^{n} a_{ij}\left(\dot{\boldsymbol{\sigma}}_i - \dot{\boldsymbol{\sigma}}_j\right) - \mu_1 \operatorname{sig}^{\varphi_1}\left\{\sum_{j=1}^{n} a_{ij}\left[\left(\boldsymbol{\sigma}_i - \hat{\boldsymbol{\sigma}}_i\right) - \left(\boldsymbol{\sigma}_j - \hat{\boldsymbol{\sigma}}_i\right)\right] + \left(\boldsymbol{\sigma}_i - \hat{\boldsymbol{\sigma}}_i\right)\right\}, \\ &= -\mu_2 \operatorname{sig}^{\varphi_2}\left\{\sum_{j=1}^{n} a_{ij}\left[\left(\boldsymbol{\sigma}_i - \hat{\boldsymbol{\sigma}}_i\right) - \left(\boldsymbol{\sigma}_j - \hat{\boldsymbol{\sigma}}_i\right)\right] + \left(\boldsymbol{\sigma}_i - \hat{\boldsymbol{\sigma}}_i\right)\right\}.\end{aligned} \tag{27}$$

It was proven that the states $\hat{\mathbf{v}}_i$ are bounded in (18); moreover, $\dot{\hat{\mathbf{v}}}_i$, $\dot{\sigma}_{ri}$, and $\ddot{\sigma}_{ri}$ are bounded from (13) and (27).

Construct another auxiliary variable $\mathbf{s}_i$ as

$$\mathbf{s}_i = \dot{\boldsymbol{\sigma}}_i - \dot{\boldsymbol{\sigma}}_{ri}. \tag{28}$$

By Property 2, we obtain

$$\mathbf{M}_i(\boldsymbol{\sigma}_i)\ddot{\boldsymbol{\sigma}}_{ri} + \mathbf{C}_i(\boldsymbol{\sigma}_i, \dot{\boldsymbol{\sigma}}_i)\dot{\boldsymbol{\sigma}}_{ri} = \mathbf{Y}_i(\boldsymbol{\sigma}_i, \dot{\boldsymbol{\sigma}}_i, \ddot{\boldsymbol{\sigma}}_{ri}, \dot{\boldsymbol{\sigma}}_{ri})\Theta_i. \tag{29}$$

And $\mathbf{Y}_i = \mathbf{Y}_i(\sigma_i, \dot{\sigma}_i, \ddot{\sigma}_{ri}, \dot{\sigma}_{ri})$ is bounded for bounded states $\ddot{\sigma}_{ri}$ and $\dot{\sigma}_{ri}$.

Combined with (5), the following is obtained:

$$\mathbf{M}_i(\boldsymbol{\sigma}_i)\dot{s}_i + \mathbf{C}_i(\boldsymbol{\sigma}_i, \dot{\boldsymbol{\sigma}}_i)\mathbf{s}_i = \boldsymbol{\tau}_i + \mathbf{d}_i - \mathbf{Y}_i\Theta_i. \tag{30}$$

The coordinated attitude tracking control law for the ith follower spacecraft is designed as

$$\begin{aligned}\boldsymbol{\tau}_i = {} & \mathbf{C}_i(\boldsymbol{\sigma}_i, \dot{\boldsymbol{\sigma}}_i)\mathbf{s}_i + \mathbf{Y}_i\hat{\Theta}_i - \kappa_1\mathbf{M}_i(\boldsymbol{\sigma}_i)\operatorname{sig}^p(\mathbf{s}_i) \\ & -\kappa_2\mathbf{M}_i(\boldsymbol{\sigma}_i)\operatorname{sig}^q(\mathbf{s}_i) - \hat{k}_i\operatorname{sgn}\left[\mathbf{s}_i^T\mathbf{M}_i^{-1}(\boldsymbol{\sigma}_i)\right]^T,\end{aligned} \tag{31}$$

$$\dot{\hat{\Theta}}_i = \mathbf{Y}_i^T\left[\mathbf{M}_i^{-T}(\boldsymbol{\sigma}_i)\right]\mathbf{s}_i, \tag{32}$$

$$\dot{\hat{k}}_i = \left\|\mathbf{s}_i^T\mathbf{M}_i^{-1}(\boldsymbol{\sigma}_i)\right\|_1, \tag{33}$$

where $\kappa_1 > 0$, $\kappa_2 > 0$, $0 < p < 1$, and $q > 1$. $\hat{\Theta}_i$ and $\hat{k}_i$ are the estimates of Θ_i and k_i, respectively.

Remark 2. It is proven in Theorem 1 that $\tilde{\sigma}_i$ and $\tilde{\mathbf{v}}_i$ converge to zero in a fixed time, which means $\hat{\sigma}_i = \sigma_0$ and $\hat{\mathbf{v}}_i = \dot{\sigma}_0$ in a fixed time; thus, after T_1, $\dot{\sigma}_{ri}$ is equivalent to

$$\begin{aligned}\mathbf{q}_i = {} & \dot{\boldsymbol{\sigma}}_0 - \sum_{j=1}^{n} a_{ij}\left(\dot{\boldsymbol{\sigma}}_i - \dot{\boldsymbol{\sigma}}_j\right) - \mu_1 \operatorname{sig}^{\varphi_1} \\ & \cdot \left\{\sum_{j=1}^{n} a_{ij}\left[\left(\boldsymbol{\sigma}_i - \boldsymbol{\sigma}_0\right) - \left(\boldsymbol{\sigma}_j - \boldsymbol{\sigma}_0\right)\right] + \left(\boldsymbol{\sigma}_i - \boldsymbol{\sigma}_0\right)\right\} \\ & - \mu_2 \operatorname{sig}^{\varphi_2}\left\{\sum_{j=1}^{n} a_{ij}\left[\left(\boldsymbol{\sigma}_i - \boldsymbol{\sigma}_0\right) - \left(\boldsymbol{\sigma}_j - \boldsymbol{\sigma}_0\right)\right] + \left(\boldsymbol{\sigma}_i - \boldsymbol{\sigma}_0\right)\right\} \\ = {} & \dot{\boldsymbol{\sigma}}_0 - \sum_{j=1}^{n} a_{ij}\mathbf{e}_{2ij} - k_1\operatorname{sig}^{\varphi_1}(\boldsymbol{\theta}_1) - k_2\operatorname{sig}^{\varphi_2}(\boldsymbol{\theta}_1).\end{aligned} \tag{34}$$

After T_1, $\mathbf{s}_i$ is equivalent to

$$\mathbf{c}_i = \boldsymbol{\theta}_{2i} + \mu_1 \mathrm{sig}^{\varphi_1}(\boldsymbol{\theta}_{1i}) + \mu_2 \mathrm{sig}^{\varphi_2}(\boldsymbol{\theta}_{1i}). \tag{35}$$

Theorem 2. *Considering the spacecraft formation attitude system (5) under an undirected connected communication graph $\overline{\mathbf{G}}$, control law (31) combined with estimators (12) and (13) guarantee the attitude errors $\mathbf{e}_1$ and $\mathbf{e}_2$ converge to the regions $\|\mathbf{e}_1\| \le \sqrt{3\sum_{i=1}^{n}\Delta_{\theta_{1i}}^2/\lambda min[(\mathbf{L}+\mathbf{I}_n)^T(\mathbf{L}+\mathbf{I}_n)]}$ and $\|\mathbf{e}_2\| \le \sqrt{3\sum_{i=1}^{n}\Delta_{\theta_{2i}}^2/\lambda min[(\mathbf{L}+\mathbf{I}_n)^T(\mathbf{L}+\mathbf{I}_n)]}$ in the fixed time $T = T_1 + T_2 + T_3$, respectively.*

Proof. First, we prove the boundedness of the system-related variables and define $\widetilde{\Theta}_i = \widehat{\Theta}_i - \Theta_i$ and $\widetilde{k}_i = k_i - \widehat{k}_i$. τ, $\mathbf{s}$, $\mathbf{d}$, $\widehat{\mathbf{k}}$, and $\widetilde{\Theta}$ are column stack vectors of τ_i, $\mathbf{s}_i$, $\mathbf{d}_i$, $\widehat{k}_i$, and $\widetilde{\Theta}_i$, respectively. $\mathbf{C}(\sigma,\dot{\sigma})$, $\mathbf{M}(\sigma)$, and $\mathbf{Y}$ are block diagonal matrices of $\mathbf{C}_i(\sigma_i,\dot{\sigma}_i)$, $\mathbf{M}_i(\sigma_i)$, and $\mathbf{Y}_i$, respectively. Substituting (31), (32), and (33) into (30), the system can be expressed in the following form:

$$\begin{aligned}\mathbf{M}(\boldsymbol{\sigma})\dot{s} = &-\kappa_1\mathbf{M}(\boldsymbol{\sigma})\mathrm{sig}^p(\mathbf{s}) - \kappa_2\mathbf{M}(\boldsymbol{\sigma})\mathrm{sig}^q(\mathbf{s}) \\ &- \widehat{k}\otimes\mathbf{I}_3\mathrm{sign}\left[\mathbf{s}^T\mathbf{M}^{-1}(\boldsymbol{\sigma})\right]^T + \mathbf{Y}\widetilde{\Theta} + \mathbf{d}.\end{aligned} \tag{36}$$

The Lyapunov function candidate V_2 is denoted as

$$V_2 = \frac{1}{2}\mathbf{s}^T\mathbf{s} + \frac{1}{2}\widetilde{\Theta}^T\widetilde{\Theta} + \frac{1}{2}\sum_{i=1}^{n}\widetilde{k}_i^2. \tag{37}$$

Taking the time derivative of the Lyapunov function V_2, we have

$$\begin{aligned}\dot{V}_2 &= \mathbf{s}^T\dot{s} + \widetilde{\Theta}^T\dot{\widetilde{\Theta}} + \sum_{i=1}^{n}\widetilde{k}_i\dot{\widetilde{k}}_i \\ &= \mathbf{s}^T\mathbf{M}^{-1}(\boldsymbol{\sigma})\left\{-\kappa_1\mathbf{M}(\boldsymbol{\sigma})\mathrm{sig}^p(\mathbf{s}) - \kappa_2\mathbf{M}(\boldsymbol{\sigma})\mathrm{sig}^q(\mathbf{s}) - \widehat{k}\otimes\mathbf{I}_3\mathrm{sgn}\left[\mathbf{s}^T\mathbf{M}^{-1}(\boldsymbol{\sigma})\right]^T + \mathbf{Y}\widetilde{\Theta} + \mathbf{d}\right\} - \widetilde{\Theta}^T\dot{\widehat{\Theta}} - \sum_{i=1}^{n}\widetilde{k}_i\dot{\widehat{k}}_i \\ &= -\kappa_1\mathbf{s}^T\mathrm{sig}^p(\mathbf{s}) - \kappa_2\mathbf{s}^T\mathrm{sig}^q(\mathbf{s}) + \widetilde{\Theta}^T\left\{\mathbf{Y}^T\left[\mathbf{M}^{-T}(\boldsymbol{\sigma})\right]\mathbf{s} - \dot{\widehat{\Theta}}\right\} - \sum_{i=1}^{n}\widehat{k}_i\left\|\mathbf{s}_i^T\mathbf{M}_i^{-1}(\boldsymbol{\sigma}_i)\right\|_1 - \sum_{i=1}^{n}\widetilde{k}_i\dot{\widehat{k}}_i + \mathbf{s}^T\mathbf{M}^{-1}(\boldsymbol{\sigma})\mathbf{d} \\ &= -\kappa_1\mathbf{s}^T\mathrm{sig}^p(\mathbf{s}) - \kappa_2\mathbf{s}^T\mathrm{sig}^q(\mathbf{s}) - \sum_{i=1}^{n}\widehat{k}_i\left\|\mathbf{s}_i^T\mathbf{M}_i^{-1}(\boldsymbol{\sigma}_i)\right\|_1 - \sum_{i=1}^{n}\widetilde{k}_i\left\|\mathbf{s}_i^T\mathbf{M}_i^{-1}(\boldsymbol{\sigma}_i)\right\|_1 + \mathbf{s}^T\mathbf{M}^{-1}(\boldsymbol{\sigma})\mathbf{d} \\ &\le -\kappa_1\mathbf{s}^T\mathrm{sig}^p(\mathbf{s}) - \kappa_2\mathbf{s}^T sig^q(\mathbf{s}).\end{aligned} \tag{38}$$

This completes the proof of the boundedness of $\mathbf{s}$, $\widetilde{\Theta}$, and $\widetilde{\mathbf{k}}$.

Second, we prove the fixed-time stability of (36). The Lyapunov function V_3 is described as

$$V_3 = \frac{1}{2}\mathbf{s}^T\mathbf{s}. \tag{39}$$

Taking the time derivative of the Lyapunov function V_3, based on Lemma 4 and Lemma 5, we have

$$\begin{aligned}\dot{V}_3 &= \mathbf{s}^T\dot{s} \\ &= \mathbf{s}^T\mathbf{M}^{-1}(\boldsymbol{\sigma})\left[-\kappa_1\mathbf{M}(\boldsymbol{\sigma})\mathrm{sig}^p(\mathbf{s}) - \kappa_2\mathbf{M}(\boldsymbol{\sigma})\mathrm{sig}^q(\mathbf{s}) - \widehat{k}\otimes\mathbf{I}_3\mathrm{sgn}\left[\mathbf{s}^T\mathbf{M}^{-1}(\boldsymbol{\sigma})\right] + \mathbf{Y}\widetilde{\Theta} + \mathbf{d}\right] \\ &= -\kappa_1\mathbf{s}^T\mathrm{sig}^p(\mathbf{s}) - \kappa_2\mathbf{s}^T\mathrm{sig}^q(\mathbf{s}) + \mathbf{s}^T\mathbf{M}^{-1}(\boldsymbol{\sigma})\mathbf{Y}\widetilde{\Theta} - \sum_{i=1}^{n}\widehat{k}_i\left\|\mathbf{s}_i^T\mathbf{M}_i^{-1}(\boldsymbol{\sigma}_i)\right\|_1 + \mathbf{s}^T\mathbf{M}^{-1}(\boldsymbol{\sigma})\mathbf{d} \\ &= -\kappa_1\mathbf{s}^T\mathrm{sig}^p(\mathbf{s}) - \kappa_2\mathbf{s}^T\mathrm{sig}^q(\mathbf{s}) - \sum_{i=1}^{n}\left\|\mathbf{s}_i^T\mathbf{M}_i^{-1}(\boldsymbol{\sigma}_i)\right\|_1^2 + \mathbf{s}^T\mathbf{M}^{-1}(\boldsymbol{\sigma})(\mathbf{Y}\widetilde{\Theta} + \mathbf{d}) \\ &\le -\kappa_1\mathbf{s}^T\mathrm{sig}^p(\mathbf{s}) - \kappa_2\mathbf{s}^T\mathrm{sig}^q(\mathbf{s}) - \sum_{i=1}^{n}\left\|\mathbf{s}_i^T\mathbf{M}_i^{-1}(\boldsymbol{\sigma}_i)\right\|_1^2 + \left[\mathbf{s}^T\mathbf{M}^{-1}(\boldsymbol{\sigma})\right]^T\left[\mathbf{s}^T\mathbf{M}^{-1}(\boldsymbol{\sigma})\right] + [(\mathbf{Y}\widetilde{\Theta} + \mathbf{d})]^T[(\mathbf{Y}\widetilde{\Theta} + \mathbf{d})] \\ &\le -\kappa_1\mathbf{s}^T\mathrm{sig}^p(\mathbf{s}) - \kappa_2\mathbf{s}^T\mathrm{sig}^q(\mathbf{s}) - \sum_{i=1}^{n}\left\|\mathbf{s}_i^T\mathbf{M}_i^{-1}(\boldsymbol{\sigma}_i)\right\|_1^2 + \sum_{i=1}^{n}\left\|\mathbf{s}_i^T\mathbf{M}_i^{-1}(\boldsymbol{\sigma}_i)\right\|^2 + \sum_{i=1}^{n}\left\|\mathbf{Y}_i\widetilde{\Theta}_i + \mathbf{d}_i\right\|^2 \\ &\le -\kappa_1\mathbf{s}^T\mathrm{sig}^p(\mathbf{s}) - \kappa_2\mathbf{s}^T\mathrm{sig}^q(\mathbf{s}) + \sum_{i=1}^{n}\left\|\mathbf{Y}_i\widetilde{\Theta}_i + \mathbf{d}_i\right\|^2 \\ &= -\kappa_1\sum_{i=1}^{n}\sum_{m=1}^{3}\left(s_{im}^2\right)^{(p+1)/2} - \kappa_2\sum_{i=1}^{n}\sum_{I=1}^{3}\left(s_{im}^2\right)^{(q+1)/2} + \sum_{i=1}^{n}\left\|\mathbf{Y}_i\widetilde{\Theta}_i + \mathbf{d}_i\right\|^2 \\ &\le -\kappa_1\left[\sum_{i=1}^{n}\sum_{m=1}^{3}\left(s_{im}^2\right)\right]^{(p+1)/2} - \kappa_2(3n)^{(1-q)/2}\left[\sum_{i=1}^{n}\sum_{m=1}^{3}\left(s_{im}^2\right)\right]^{(q+1)/2} + \sum_{i=1}^{n}\left\|\mathbf{Y}_i\widetilde{\Theta}_i + \mathbf{d}_i\right\|^2.\end{aligned} \tag{40}$$

Since $\mathbf{Y}_i$, $\widetilde{\Theta}_i$, and $\mathbf{d}_i$ are bounded, there exist a constant η such that

$$\sum_{i=1}^{n} \left\| \mathbf{Y}_i \widetilde{\Theta}_i + \mathbf{d}_i \right\|^2 \leq \eta. \tag{41}$$

Then, we obtain

$$\dot{V}_3 \leq -\left[(1-\varsigma_1)\kappa_1 2^{(p+1)/2} - \frac{\eta}{V_3^{(p+1)/2}} \right] V_3^{(p+1)/2} - \varsigma_1 \kappa_1 2^{(p+1)/2} V_3^{(p+1)/2} - \kappa_2 2^{(q+1)/2} (3n)^{(1-q)/2} V_3^{(q+1)/2}, \tag{43}$$

$$\dot{V}_3 \leq -\kappa_1 2^{(p+1)/2} V_3^{(p+1)/2} - \left[(1-\varsigma_2)\kappa_2 2^{(q+1)/2} (3n)^{(1-q)/2} - \frac{\eta}{V_3^{(q+1)/2}} \right] V_3^{(q+1)/2} - \varsigma_2 \kappa_2 2^{(q+1)/2} (3n)^{(1-q)/2} V_3^{(q+1)/2}, \tag{44}$$

where $\varsigma_1 = \varsigma_2 = 0.5$.

From (43), if $(1-\varsigma_1)\kappa_1 2^{(p+1)/2} - \eta/V_3^{(p+1)/2} > 0$, then the fixed-time stability is guaranteed. By Lemma 3, auxiliary variable $\mathbf{s}$ converges to the region $\|\mathbf{s}\| \leq [\eta/[(1-\varsigma_1)]\kappa_1]^{1/(p+1)}$ in fixed-time $T_{21} \leq 2^{(1-p)/2}/\varsigma_1\kappa_1(1-p) + (2/3n)^{(1-q)/2}/\kappa_2(q-1)$. From (44), if $(1-\varsigma_2)\kappa_2 2^{(q+1)/2}$ $(3n)^{(1-q)/2} - \eta/V_3^{(q+1)/2} > 0$, auxiliary variable $\mathbf{s}$ converges to the region $\|\mathbf{s}\| \leq [\eta/(1-\varsigma_2)$ $\kappa_2(3n)^{(1-q)/2}]^{1/(q+1)}$ in fixed time $T_{22} \leq 2^{(1-p)/2}/\kappa_1(1-p) + (2/$ $3n)^{(1-q)/2}/\varsigma_2\kappa_2(q-1)$. Then, the auxiliary variable $\mathbf{s}$ converges to the region:

$$\dot{V}_3 \leq -\kappa_1 2^{(p+1)/2} V_3^{(p+1)/2} - \kappa_2 2^{(q+1)/2} (3n)^{(1-q)/2} V_3^{(q+1)/2} + \eta. \tag{42}$$

Here, (42) is rewritten as the following two equations:

$$\|\mathbf{s}\| \leq \Delta = \min\left\{ \left[\frac{\eta}{(1-\varsigma_1)\kappa_1} \right]^{1/(1+p)}, \left[\frac{\eta}{(1-\varsigma_2)\kappa_2 (3n)^{(1-q)/2}} \right]^{1/(q+1)} \right\}, \tag{45}$$

which means $|s_{im}| \leq \Delta$, where $i = 1, 2, \ldots, n$ and $m = 1, 2, 3$, in a fixed time as

$$T_2 = \max(T_{21}, T_{22}) = \max\left[\frac{2^{(1-p)/2}}{\varsigma_1\kappa_1(1-p)} + \frac{(2/3n)^{(1-q)/2}}{\kappa_2(q-1)}, \frac{2^{(1-p)/2}}{\varsigma_1\kappa_1(1-p)} + \frac{(2/3n)^{(1-q)/2}}{\kappa_2(q-1)} \right]. \tag{46}$$

Therefore, we obtain the following equations after $T_1 + T_2$:

$$s_{im} = c_{im} = \theta_{2im} + \mu_1 \mathrm{sig}^{\varphi_1}(\theta_{1im}) + \mu_2 \mathrm{sig}^{\varphi_2}(\theta_{1im}) = \phi_{im}, |\phi_{im}| \leq \Delta, \tag{47}$$

$$\begin{aligned} \theta_{2im} &= -\mu_1 \mathrm{sig}^{\varphi_1}(\theta_{1im}) - \mu_2 \mathrm{sig}^{\varphi_2}(\theta_{1im}) + \phi_{im} \\ &\leq -\mu_1 \mathrm{sig}^{\varphi_1}(\theta_{1im}) - \mu_2 \mathrm{sig}^{\varphi_2}(\theta_{1im}) + \Delta. \end{aligned} \tag{48}$$

The Lyapunov function candidate V_4 is denoted as

$$V_4 = \frac{1}{2}\theta_{1\mathrm{im}}^2. \tag{49}$$

Taking the time derivative of the Lyapunov function V_4, we have

$$\begin{aligned} \dot{V}_4 &= \theta_{1im}\theta_{2im} \\ &= -\mu_1 2^{(\varphi_1+1)/2} \left[\frac{1}{2}(\theta_{1im})^2 \right]^{(\varphi_1+1)/2} - \mu_2 2^{(\varphi_2+1)/2} \left[\frac{1}{2}(\theta_{1im})^2 \right]^{(\varphi_2+1)/2} + \phi_{im}\theta_{1im} \\ &\leq -\mu_1 2^{(\varphi_1+1)/2} V_4^{(\varphi_1+1)/2} - \mu_2 2^{(\varphi_2+1)/2} V_4^{(\varphi_2+1)/2} + \Delta|\theta_{1im}|. \end{aligned} \tag{50}$$

Similar to the analysis of V_3, $\dot{V}_4 \leq -\mu_1 2^{(\varphi_1+1)/2} V_4^{(\varphi_1+1)/2} - \mu_2 2^{(\varphi_1+1)/2} V_4^{(\varphi_2+1)/2} + \Delta|\theta_{1im}|$ can be rewritten as the following two equations:

$$\dot{V}_4 \leq -\left[(1-\varsigma_1)\mu_1 2^{(\varphi_1+1)/2} - \frac{\Delta|\theta_{1im}|}{V_4^{(\varphi_1+1)/2}}\right] V_4^{(\varphi_1+1)/2} - \varsigma_1 \mu_1 2^{(\varphi_1+1)/2} V_4^{(\varphi_1+1)/2} - \mu_2 2^{(\varphi_2+1)/2} V_4^{(\varphi_2+1)/2}, \tag{51}$$

$$\dot{V}_4 \leq -\left[(1-\varsigma_2)\mu_2 2^{(\varphi_2+1)/2} - \frac{\Delta|\theta_{1im}|}{V_4^{(\varphi_2+1)/2}}\right] V_4^{(\varphi_2+1)/2} - \mu_1 2^{(\varphi_2+1)/2} V_4^{(\varphi_2+1)/2} - \varsigma_2 \mu_2 2^{(\varphi_2+1)/2} V_4^{(\varphi_2+1)/2}. \tag{52}$$

From (51), if $(1-\varsigma_1)\mu_1 2^{(\varphi_1+1)/2} - \Delta|\theta_{1im}|/V_4^{(\varphi_1+1)/2} > 0$, then the fixed-time stability is guaranteed. By Lemma 3, the lumped attitude state error θ_{1im} converges to the region $|\theta_{1im}| \leq [\Delta/(1-\varsigma_1)\mu_1]^{1/\varphi_1}$ in fixed time $T_{31} \leq 2^{(1-\varphi_1)/2}/\varsigma_1\mu_1(1-\varphi_1) + 2^{(1-\varphi_1)/2}/u_2(\varphi_2-1)$. From (52), if $(1-\varsigma_2)\mu_2 2^{(\varphi_1+1)/2} - \Delta|\theta_{1im}|/V_4^{(\varphi_2+1)/2} > 0$, the lumped attitude state error θ_{1im} converges to the region $|\theta_{1im}| \leq (\Delta/(1-\varsigma_2)\mu_2)^{1/\varphi_2}$ in fixed time $T_{32} \leq 2^{(1-\varphi_1)/2}/\mu_1(1-\varphi_1) + 2^{(1-\varphi_1)/2}/\varsigma_2 u_2(\varphi_2-1)$. Then, the lumped attitude state error θ_{1im} converges to the region:

$$|\theta_{1im}| \leq \Delta_{\theta_{1i}} = \min\left[\left(\frac{\Delta}{(1-\varsigma_1)\mu_1}\right)^{1/\varphi_1}, \left(\frac{\Delta}{(1-\varsigma_2)\mu_2}\right)^{1/\varphi_2}\right]. \tag{53}$$

Based on (48), the lumped attitude state error θ_{2im} converges to the region:

$$|\theta_{2im}| \leq \mu_1|\theta_{1im}|^{\varphi_1} + \mu_2|\theta_{1im}|^{\varphi_2} + \Delta = \mu_1\Delta_{\theta_{1i}}^{\varphi_1} + \mu_2\Delta_{\theta_{1i}}^{\varphi_2} + \Delta = \Delta_{\theta_{2i}}. \tag{54}$$

Moreover, the settling time of θ_{1im} and θ_{2im} is

$$T_3 = \max(T_{31}, T_{32}) = \max\left[\frac{2^{(1-\varphi_1)/2}}{\varsigma_1\mu_1(1-\varphi_1)} + \frac{2^{(1-\varphi_2)/2}}{u_2(\varphi_2-1)}, \frac{2^{(1-\varphi_1)/2}}{\mu_1(1-\varphi_1)} + \frac{2^{(1-\varphi_2)/2}}{\varsigma_2 u_2(\varphi_2-1)}\right]. \tag{55}$$

Therefore, after $T_1 + T_2 + T_3$, we obtain

$$\lambda\min\left[(\mathbf{L}+\mathbf{I}_n)^T(\mathbf{L}+\mathbf{I}_n)\right]\mathbf{e}_1^T\mathbf{e}_1 \leq \mathbf{e}_1^T\left[(\mathbf{L}+\mathbf{I}_n)\otimes\mathbf{I}_3\right]^T\left[(\mathbf{L}+\mathbf{I}_n)\otimes\mathbf{I}_3\right]\mathbf{e}_1 = \boldsymbol{\theta}_1^T\boldsymbol{\theta}_1 \leq 3\sum_{i=1}^{n}\Delta_{\theta_{1i}}^2, \tag{56}$$

$$\lambda\min\left[(\mathbf{L}+\mathbf{I}_n)^T(\mathbf{L}+\mathbf{I}_n)\right]\mathbf{e}_2^T\mathbf{e}_2 \leq \mathbf{e}_2^T\left[(\mathbf{L}+\mathbf{I}_n)\otimes\mathbf{I}_3\right]^T\left[(\mathbf{L}+\mathbf{I}_n)\otimes\mathbf{I}_3\right]\mathbf{e}_2 = \boldsymbol{\theta}_2^T\boldsymbol{\theta}_2 \leq 3\sum_{i=1}^{n}\Delta_{\theta_{2i}}^2. \tag{57}$$

Then, the attitude state errors $\mathbf{e}_1$ and $\mathbf{e}_2$ converge to the regions:

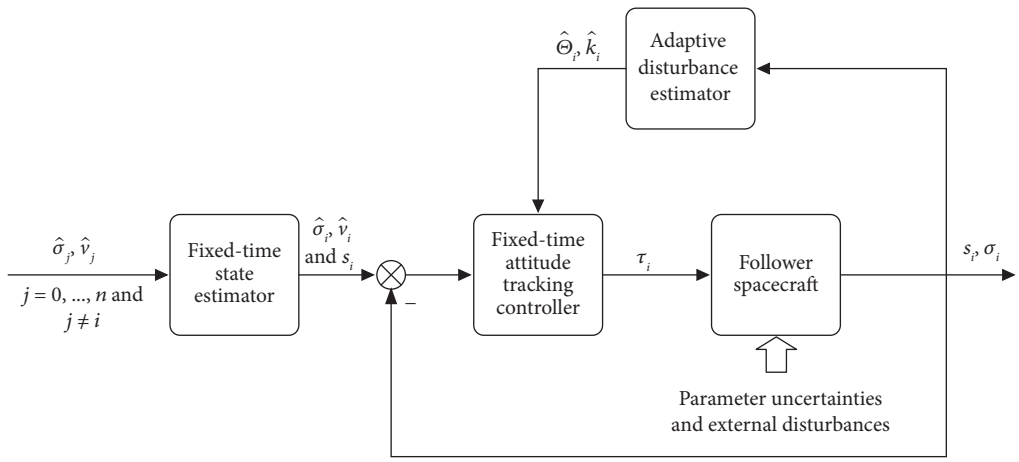

Figure 1: The control system schematic diagram of the ith spacecraft.

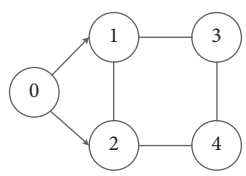

Figure 2: Communication topology.

Table 1: Initial parameters of follower spacecrafts.

Spacecraft no. i	Inertia matrix $\mathbf{J}_i$ (kg · m^2)	Initial attitude $\sigma_i(0)$	Initial attitude derivative $\dot{\sigma}_i(0)$
1	[15 0.4 1; 0.4 14 1.5; 1 1.5 12]	[−0.0462, 0.0215, 0.050]	[0, 0, 0]
2	[14 0.3 1; 0.3 16 1.3; 1 1.3 15]	[0.0542, 0.0114, −0.0548]	[0, 0, 0]
3	[18 0.5 2; 0.5 13 1.6; 2 1.6 14]	[0.0495, −0.0641, 0.0067]	[0, 0, 0]
4	[16 0.6 1; 0.6 15 1.4; 1 1.4 17]	[0.0335, 0.0414, −0.0322]	[0, 0, 0]

$$\|\mathbf{e}_1\| \leq \sqrt{\frac{3\sum_{i=1}^{n}\Delta_{\theta_{1i}}^2}{\lambda\min\left[\left(\mathbf{L}+\mathbf{I}_n\right)^T\left(\mathbf{L}+\mathbf{I}_n\right)\right]}}, \tag{58}$$

$$\|\mathbf{e}_2\| \leq \sqrt{\frac{3\sum_{i=1}^{n}\Delta_{\theta_{2i}}^2}{\lambda\min\left[\left(\mathbf{L}+\mathbf{I}_n\right)^T\left(\mathbf{L}+\mathbf{I}_n\right)\right]}}, \tag{59}$$

in fixed time $T = T_1 + T_2 + T_3$, respectively. This completes the proof of Theorem 2. □

Remark 3. The controller proposed in this study contains several parameters, where $0 < \gamma_1 < 1$, $0 < p < 1$, $0 < \mu_1 < 1$, and $0 < \varphi_1 < 1$ affect the convergence accuracy of the system. The smaller the values of γ_1, p, μ_1, and φ_1, the higher the accuracy of the estimator and the control performance; however, smaller values cause the system to produce larger chattering. $\gamma_2 > 1$, $q > 1$, $\mu_2 > 1$, and $\varphi_2 > 1$ affect the control system response speed; the larger the values of γ_2, q, μ_2, and φ_2 are, the higher the obtained system response speed is; however, large values will cause a large overshoot.

As shown in Figure 1, the control system designed in this study includes fixed-time state observers, fixed-time attitude tracking controllers, and adaptive disturbance estimators for the ith spacecraft, where $j = 0, ..., n$ and $j \neq i$ represents the spacecraft that is available to provide the ith spacecraft with the attitude information.

4. Simulation Results

In this section, to demonstrate the validity of the proposed control algorithms, numerical simulations for a spacecraft formation system are conducted, and the communication topology is described in Figure 2. A system consisting of four follower spacecraft and one leader spacecraft satisfies Assumption 1. Table 1 lists the inertia matrix and initial conditions of the follower spacecraft. To obtain better control performance in the simulation process, after several debugging operations, the parameters of the distributed estimator in (12) and (13) and the auxiliary variable $\dot{\sigma}_{ri}$ and the control law (31) are set as $\alpha_1 = 1$, $\alpha_2 = 1$, $\kappa_1 = 1$, $\kappa_2 = 0.8$, $\gamma_1 = 0.8$, $\gamma_2 = 1.2$, $\mu_1 = 0.4$, $\mu_2 = 1.2$, $\varphi_1 = 0.5$, $\varphi_2 = 1.5$, $p = 0.4$, and $q = 1.3$, respectively. The additional variation

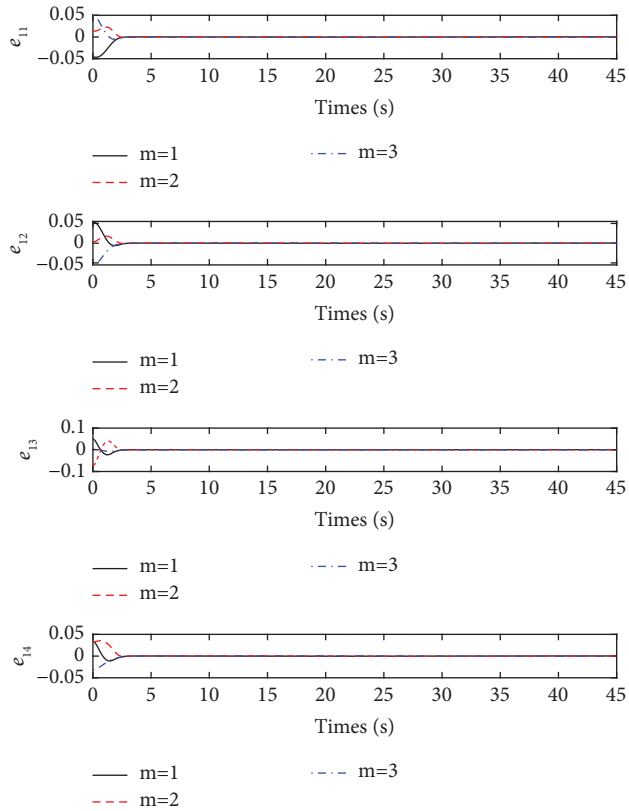

Figure 3: Attitude tracking errors $\mathbf{e}_{1i}$.

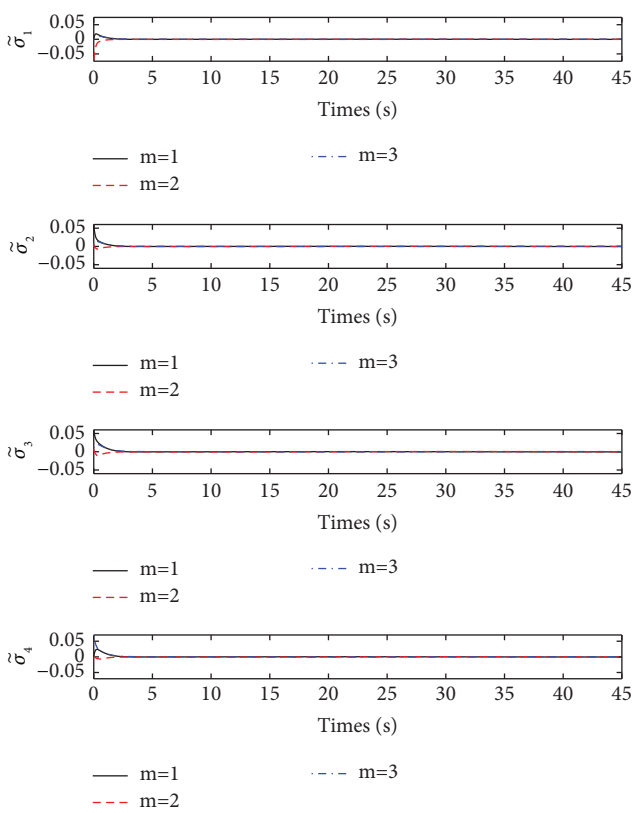

Figure 4: Estimation errors $\tilde{\sigma}_i$.

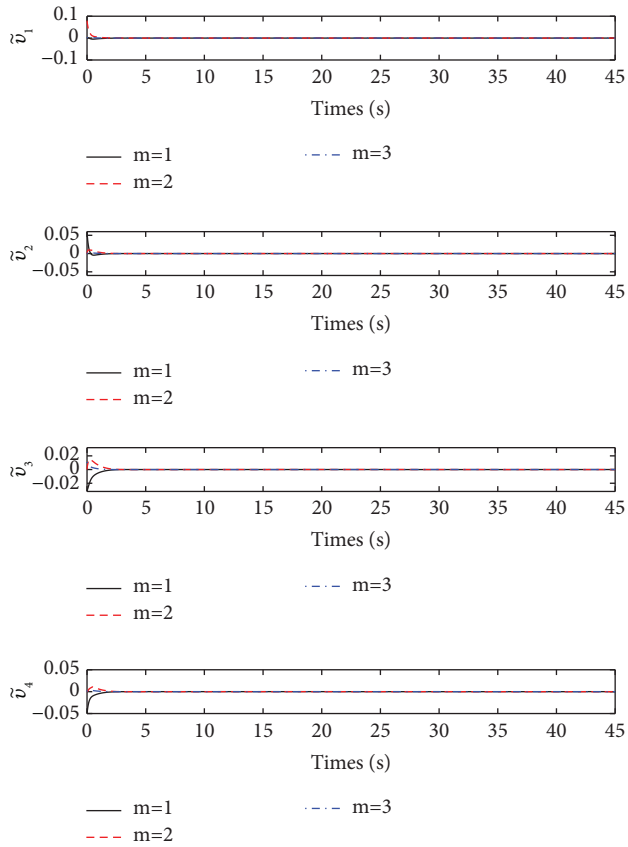

Figure 5: Estimation errors $\tilde{\mathbf{v}}_i$.

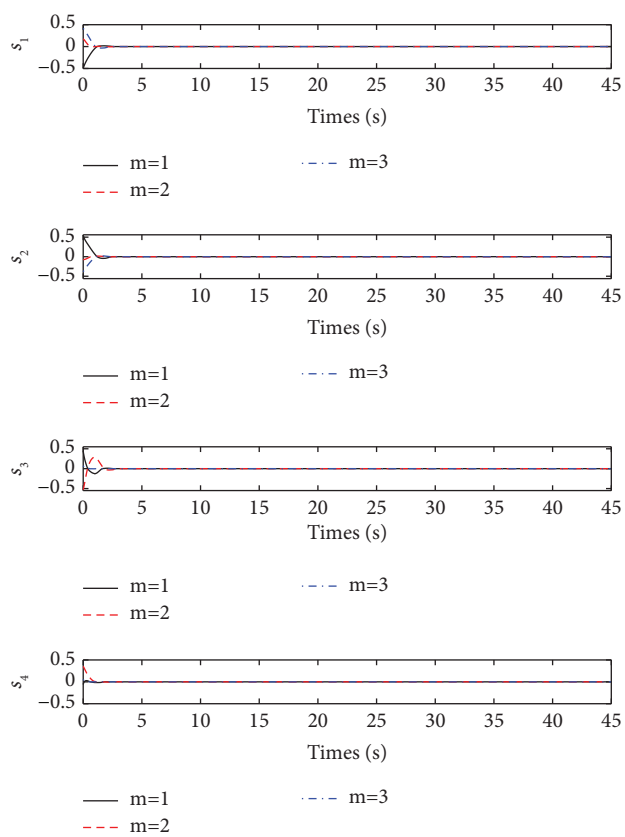

Figure 6: Auxiliary variable $\mathbf{s}_i$.

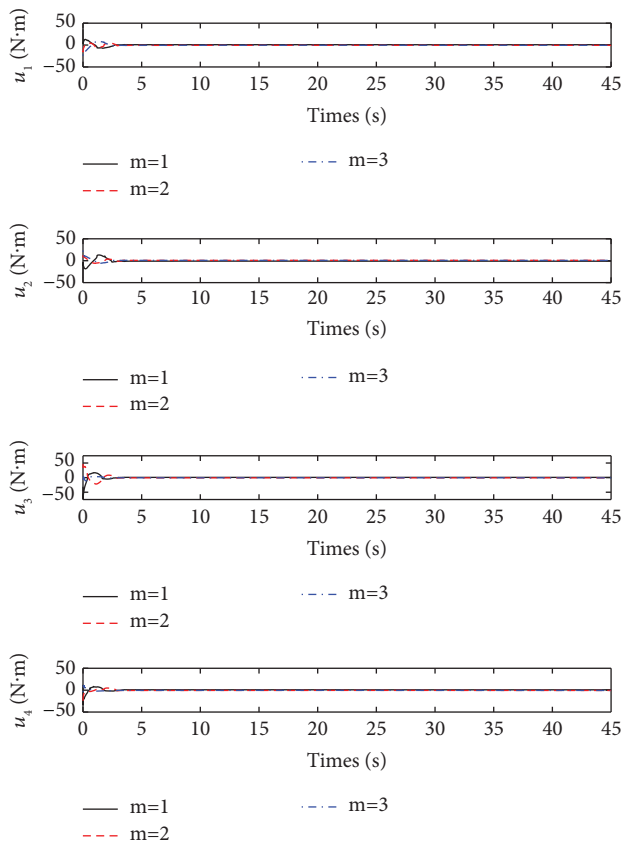

Figure 7: Control torques $\mathbf{u}_i$.

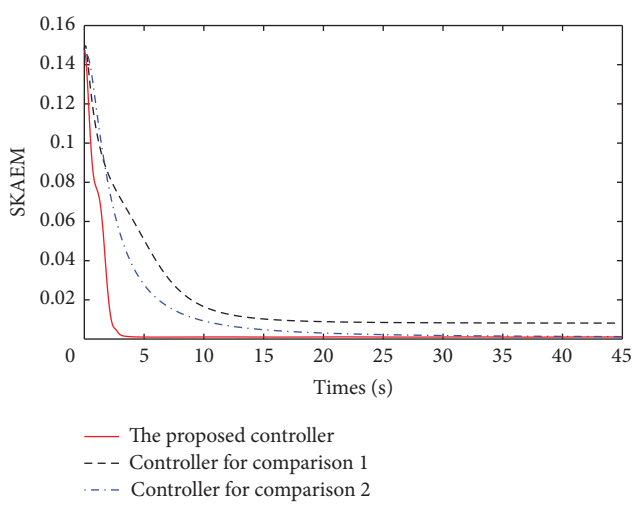

Figure 8: The control performance comparison of SKAEM.

inertia matrix for each follower spacecraft is set as $\left[-0.03\times\ \sin(0.1t)\ \ 0.04\times\ \cos(0.1t)\ \ 0.05\times\ \sin(0.1t)\right]^T$ N $\cdot$ m. The additional variation inertia matrix for each follower spacecraft is set as $\begin{bmatrix} 0.1\ \sin(0.1t) & 0.01\ \sin(0.1t) & 0.01\ \sin(0.1t) \\ 0.01\ \sin(0.1t) & 0.15\ \sin(0.1t) & 0.01\ \sin(0.1t) \\ 0.01\ \sin(0.1t) & 0.01\ \sin(0.1t) & 0.1\ \cos(0.1t) \end{bmatrix}$ kg $\cdot$m^2.

Figure 3 shows that the attitude tracking error $\mathbf{e}_i$ converges to $|e_{\mathrm{im}}| < 4\times 10^{-4}$ in four seconds in the presence of external disturbing torques and periodic changes in the inertia matrix. The estimation errors $\widetilde{\sigma}_i$ and $\widetilde{\mathbf{v}}_i$ are illustrated in Figures 4 and 5, respectively. $\widetilde{\sigma}_i$ and $\widetilde{\mathbf{v}}_i$ can converge to regions $|\widetilde{\sigma}_{\mathrm{im}}| < 4\times 10^{-4}$ and $|\widetilde{v}_{\mathrm{im}}| < 2\times 10^{-5}$ with a dynamic leader, respectively. As illustrated in Figure 6, the auxiliary variable $\mathbf{s}_i$ converges to region $|s_{\mathrm{im}}| < 2\times 10^{-4}$. Figure 7 shows the control torques of the follower spacecraft. As the desired attitude is dynamic, the control torques will never be zero, which is illustrated in Figure 7. To reflect the performance of the controller proposed in this study, comparisons are made with the controllers in [19] (the controller for comparison 1) and [23] (the controller for comparison 2). The station-keeping attitude error metric (SKAEM) is defined as SKEAM = $\sqrt{\sum_{i=1}^{n}\sum_{m=1}^{3} e_{im}^2}$. The control performance comparison is shown in Figure 8. The controller proposed in this study can provide a faster convergence rate and a more accurate attitude tracking performance.

5. Conclusion

The distributed coordinated attitude tracking control problem for a spacecraft formation system with a dynamic leader is investigated in the presence of external disturbing torques and parameter uncertainty in this study. Considering that the attitude information of the leader is only available to some of the follower spacecraft, fixed-time distributed estimators that only utilize the neighbors' information are proposed to estimate the leader's attitude information. Based on the estimated information, auxiliary variables are designed for the subsequent design. By employing the fixed-time control method, a fixed-time control algorithm combined with an adaptive control algorithm, which is used to cope with external disturbances and parameter uncertainties, is proposed. The algorithm achieves fixed-time convergence of the auxiliary variable, and the convergence time is independent of the initial condition. By employing the Lyapunov approach, the proposed control algorithms demonstrate that the attitude of each follower spacecraft can be synchronized with the attitude of the dynamic leader in a fixed time. The fixed-time control algorithm can be used to reduce the convergence time in the case of tracking a dynamic target, as the convergence time is influenced by the initial conditions, which change at all times due to the dynamic target in conventional control methods and finite-time control algorithms. The effectiveness of the proposed control algorithms is demonstrated by numerical simulations. In future work, based on this research, I will continue to deeply study the fixed-time attitude tracking control of multispacecraft formations and strive to focus on the state estimator that can be used in the case of directed graph communication.

Data Availability

The data used to support the findings of this study are included within the article.

Conflicts of Interest

The author declares that there are no conflicts of interest.

References

[1] R. Kristiansen and P. J. Nicklasson, "Spacecraft formation flying: a review and new results on state feedback control," *Acta Astronautica*, vol. 65, no. 11-12, pp. 1537–1552, 2009, https://doi.org/10.1016/j.actaastro.2009.04.014.

[2] K. Zhang and M. A. Demetriou, "Adaptation and optimization of the synchronization gains in the adaptive spacecraft attitude synchronization," *Aerospace Science and Technology*, vol. 46, no. 7, pp. 116–123, 2015.

[3] C. Ma, Q. Zeng, and X. Zhao, "Distributed adaptive attitude synchronization for spacecraft formation flying with sampled-data information flows," *Journal of the Franklin Institute*, vol. 352, no. 7, pp. 2796–2809, 2015.

[4] B. Wu, D. Wang, and E. Poh, "Decentralized sliding-mode control for attitude synchronization in spacecraft formation," *International Journal of Robust and Nonlinear Control*, vol. 23, no. 11, pp. 1183–1197, 2013.

[5] A. Abdessameud, A. Tayebi, and I. G. Polushin, "Attitude synchronization of multiple rigid bodies with communication delays," *IEEE Transactions on Automatic Control*, vol. 57, no. 9, pp. 2405–2411, 2012.

[6] D. V. Dimarogonas, P. Tsiotras, and K. J. Kyriakopoulos, "Leader–follower cooperative attitude control of multiple rigid bodies," *Systems & Control Letters*, vol. 58, no. 6, pp. 429–435, 2009.

[7] Y. Zou, "Attitude tracking control for spacecraft with robust adaptive RBFNN augmenting sliding mode control," *Aerospace Science and Technology*, vol. 56, no. 9, pp. 197–204, 2016.

[8] Q. Wang and C. Sun, "Distributed asymptotic consensus in directed networks of nonaffine systems with nonvanishing disturbance," *IEEE/CAA Journal of Automatica Sinica*, vol. 8, no. 6, pp. 1133–1140, 2021.

[9] Q. Wang, H. E. Psillakis, and C. Sun, "Adaptive cooperative control with guaranteed convergence in time-varying networks of nonlinear dynamical systems," *IEEE Transactions on Cybernetics*, vol. 50, no. 12, pp. 5035–5046, 2020.

[10] J. Zhang, G. Yan, Q. Hu, and D. Wang, "Finite-time attitude synchronization for spacecraft formation flying via output feedback," in *Proceedings of the 33rd Chinese Control Conference*, pp. 1638–1643, IEEE, Nanjing, China, July 2014.

[11] A. M. Zou and K. D. Kumar, "Distributed attitude coordination control for spacecraft formation flying," *IEEE Transactions on Aerospace and Electronic Systems*, vol. 48, no. 2, pp. 1329–1346, 2012.

[12] S. Mobayen, K. A. Alattas, and W. Assawinchaichote, "Adaptive continuous barrier function terminal sliding mode control technique for disturbed robotic manipulator," *IEEE Transactions on Circuits and Systems I: Regular Papers*, vol. 68, no. 10, pp. 4403–4412, 2021.

[13] O. Mofid, S. Mobayen, C. Zhang, and B. Esakki, "Desired tracking of delayed quadrotor UAV under model uncertainty and wind disturbance using adaptive super-twisting terminal sliding mode control," *ISA Transactions*, 2021.

[14] O. Mofid and S. Mobayen, "Adaptive finite-time backstepping global sliding mode tracker of quad-rotor UAVs under model uncertainty, wind perturbation, and input saturation," *IEEE Transactions on Aerospace and Electronic Systems*, vol. 58, no. 1, pp. 140–151, 2022.

[15] A. Polyakov, "Nonlinear feedback design for fixed-time stabilization of linear control systems," *IEEE Transactions on Automatic Control*, vol. 57, no. 8, pp. 2106–2110, 2012.

[16] B. Ning, Z. Zuo, J. Jin, and J. Zheng, "Distributed fixed-time coordinated tracking for nonlinear multi-agent systems under directed graphs," *Asian Journal of Control*, vol. 20, no. 2, pp. 646–658, 2017.

[17] C. Ton and C. Petersen, "Continuous fixed-time sliding mode control for spacecraft with flexible appendages," *IFAC-papersOnLine*, vol. 51, no. 12, pp. 1–5, 2018.

[18] J. Mei, W. Ren, and G. Ma, "Distributed containment control for Lagrangian networks with parametric uncertainties under a directed graph," *Automatica*, vol. 48, no. 4, pp. 653–659, 2012.

[19] W. S. Sui, G. R. Duan, M. Z. Hou, and M. R. Zhang, "Distributed fixed-time attitude synchronization control for multiple rigid spacecraft," *International Journal of Control, Automation and Systems*, vol. 17, no. 5, pp. 1117–1130, 2019.

[20] W. Wang, C. Li, Y. Sun, and G. Ma, "Distributed coordinated attitude tracking control for spacecraft formation with communication delays," *ISA Transactions*, vol. 85, pp. 97–106, 2019.

[21] J. Zhou, G. Ma, and Q. Hu, "Delay depending decentralized adaptive attitude synchronization tracking control of spacecraft formation," *Chinese Journal of Aeronautics*, vol. 25, no. 3, pp. 406–415, 2012.

[22] H. Liang, Z. Sun, and J. Wang, "Attitude coordination of satellite swarms with communication delays," *Aircraft Engineering & Aerospace Technology*, vol. 85, no. 3, pp. 222–235, 2013.

[23] R. Liu, J. Chu, and H. Du, "Fixed-time 6-DOF coordinated control of spacecraft formation flying," in *Proceedings of the 2021 33rd Chinese Control and Decision Conference (CCDC)*, pp. 4771–4776, IEEE, Kunming, China, May 2021.

[24] L. Zhao and Y. Jia, "Decentralized adaptive attitude synchronization control for spacecraft formation using nonsingular fast terminal sliding mode," *Nonlinear Dynamics*, vol. 78, no. 4, pp. 2779–2794, 2014.

[25] D. H. Zhai and Y. Xia, "Adaptive control of semi-autonomous teleoperation system with asymmetric time-varying delays and input uncertainties," *IEEE Transactions on Cybernetics*, vol. 47, no. 11, pp. 3621–3633, 2017.

[26] C. Godsil and G. Royle, *Algebraic Graph Theory*, Springer, New York, NY, USA, 2001.

[27] Y. Hong, J. Hu, and L. Gao, "Tracking control for multi-agent consensus with an active leader and variable topology," *Automatica*, vol. 42, no. 7, pp. 1177–1182, 2006.

[28] Z. Zuo and L. Tie, "A new class of finite-time nonlinear consensus protocols for multi-agent systems," *International Journal of Control*, vol. 87, no. 2, pp. 363–370, 2013.

[29] K. Peng and Y. Yang, "Leader-following consensus problem with a varying-velocity leader and time-varying delays," *Physica A: Statistical Mechanics and Its Applications*, vol. 388, no. 2-3, pp. 193–208, 2009.